Functional Role of a Mobile Loop of *Escherichia coli* Dihydrofolate Reductase in Transition-State Stabilization†

Luyuan Li,‡ Christopher J. Falzone,‡ Peter E. Wright,§ and Stephen J. Benkovic*,‡

Department of Chemistry, The Pennsylvania State University, University Park, Pennsylvania 16802, and Department of Molecular Biology, The Scripps Research Institute, 10666 North Torrey Pines Road, La Jolla, California 92037

Received March 2, 1992; Revised Manuscript Received May 20, 1992

ABSTRACT: The function of a highly mobile loop in *Escherichia coli* dihydrofolate reductase was studied by constructing a mutant (DL1) using cassette mutagenesis that had four residues deleted in the middle section of the loop (Met16–Ala19) and a glycine inserted to seal the gap. This part of the loop involves residues 16–20 and is disordered in the X-ray crystal structures of the apoprotein and the $NADP^+$ binary complex but forms a hairpin turn that folds over the nicotinamide moiety of $NADP^+$ and the pteridine moiety of folate in the ternary complex [Bystroff, C., & Kraut, J. (1991) *Biochemistry 30,* 2227–2239]. The steady-state and pre-steady-state kinetics and two-dimensional ^1H NMR spectra were analyzed and compared to the wild-type protein. The kinetics on the DL1 mutant enzyme show that the K_M value for NADPH (5.3 μM), the K_M for dihydrofolate (2 μM), the rate constant for the release of the product tetrahydrofolate (10.3 s^{-1}), and the intrinsic pK_a value (6.2) are similar to those exhibited by the wild-type enzyme. However, the hydride-transfer rate declines markedly from the wild-type value of 950 s^{-1} to 1.7 s^{-1} for the DL1 mutant and when taken with data for substrate binding indicates that the loop contributes to substrate flux by a factor of 3.5×10^4. Thus, the mobility of loop I may provide a mechanism of recruiting hydrophobic residues which can properly align the nicotinamide and pteridine rings for the hydride-transfer process (a form of transition-state stabilization). Two-dimensional NMR spectra show a slow (on the NMR time scale) exchange process at 298 K in the wild-type protein which cannot be detected in the deletion mutant. This slow process in the wild-type protein can be partially attributed to a two-site exchange of some of the residues in loop I. Therefore, the deletion of the hairpin-forming residues in loop I also affects the observed dynamics of the secondary structure in the wild-type protein and thus ties the changes in the kinetic behavior of the DL1 protein to the restricted movement of its loop I relative to the wild-type enzyme.

Loops are common secondary structural elements defined by a contiguous segment of polypeptide. They lack regular dihedral angles and hydrogen bond patterns and allow the protein backbone to reverse direction in three-dimensional space (Leszczynski & Rose, 1986; Richardson, 1981). Loops are variable in length and composition and are usually situated near the surface of proteins where they can play a role in ligand interaction and biological recognition. As has been pointed out (Leszczynski & Rose, 1986), loops are excellent candidates for protein engineering studies.

The role that loops play in protein stability and catalysis has been assessed in several enzyme systems by deletion of one or more loops or by loop swapping. For example, four loops in yeast iso-1-cytochrome *c* were individually deleted; two of the deletions either prevented synthesis of the protein or resulted in highly labile proteins in vivo (Fetrow et al., 1989). The other two loop deletions were better tolerated, and the proteins showed partial activity. In the example of staphylococcal nuclease, deletion of the loop next to a putative catalytic glutamyl residue (Glu43) resulted in a protein that was more stable and affected catalysis less than a single Glu43Asp mutant (Poole et al., 1991). However, deletion of a portion of a mobile loop in triosephosphate isomerase resulted in a protein with 10^{-5}-fold lower specific catalytic activity than that of the wild-type enzyme (Pompliano et al., 1990). In this case, the diminished activity stems from a higher activation barrier for the enolization of bound substrate to the product dihydroxyacetone phosphate. For the mutant enzyme, the enediol intermediate is weakly bound and is released before turnover and the decomposition products methylglyoxal and inorganic phosphate are detected. This suggests that the function of this mobile loop is to assist in the tight binding of the reactive intermediate in order to favor the production of the desired product. However, in the example of phospholipase A_2 (Kuipers et al., 1989), deletion of a surface loop gives rise to enhanced enzymatic activity and altered substrate specificity. Loops have also been reported to play a role in allosteric regulations. A loop containing catalytic residues appears essential for the stabilization of the allosteric form of the *Escherichia coli* aspartate transcarbamylase (Middleton et al., 1989). The T-state to R-state transition of glycogen phosphorylase has been proposed to involve a loop that becomes disordered. This greater flexibility apparently now allows access to the active site (Barford & Johnson, 1989).

Dihydrofolate reductase (5,6,7,8-tetrahydrofolate:$NADP^+$ oxidoreductase, EC 1.5.1.3; DHFR,[1] which catalyzes the NADPH-dependent reduction of 7,8-dihydrofolate (H_2F) to 5,6,7,8-tetrahydrofolate (H_4F), possesses a loop (loop I) which, according to X-ray crystallographic studies, is the most mobile

† Supported by National Institutes of Health Grants GM 24129 (S.J.B.) and GM 36643 (P.E.W.). C.J.F. is supported by a postdoctoral fellowship from Merck Sharp & Dohme.

‡ The Pennsylvania State University.

§ The Scripps Research Institute.

[1] Abbreviations: DHFR, dihydrofolate reductase; H_2F, 7,8-dihydrofolate; DL1, mutant *E. coli* DHFR in which residues 16–19 are replaced with one glycine residue; H_4F, 5,6,7,8-tetrahydrofolate; MTX, methotrexate; $NADP^+$, nicotinamide adenine dinucleotide phosphate; NADPH, nicotinamide adenine dinucleotide phosphate, reduced; NMN, nicotinamide mononucleotide; NOESY, nuclear Overhauser enhancement spectroscopy; ROESY (CAMELSPIN), rotating-frame nuclear Overhauser spectroscopy.

0006-2960/92/0431-7826$03.00/0

structural element in the entire enzyme molecule (Bystroff & Kraut, 1991). Loop I consists of 15 amino acid residues (residues 9–24; Volz et al., 1982); its central section, residues 16–20, is disordered in the apoenzyme and the $NADP^+$–holoenzyme crystal structures, generating an opening of the active-site cavity to solvent. NADPH binds in an extended conformation with its nicotinamide moiety inserted into the cavity with the opening now serving as an entrance for the cofactor. The binding of both folate and $NADP^+$ causes the disordered segment of the loop to form a hairpin turn defined by hydrogen bonding between the backbone carbonyl oxygen of Met16 and the amino nitrogen of Ala19. The newly formed hairpin folds over the binding sites of the nicotinamide moiety of $NADP^+$ and the pteridine moiety of folate. In addition, the loop moves upon the formation of the ternary complex toward the αC-helix, and a hydrogen bond is formed between the side chain of Asn18 and the backbone carbonyl oxygen of His45 in the helix. The hairpin then serves as a lid that closes the active-site opening in the ternary complex. The movement of loop I also causes the bending of the N-terminus of the αB-helix by about 1.5 Å toward the pteridine binding site, making the folate binding cleft tighter. As a result of the αB-helix shift, the hydrogen-bonding contacts between residues 21 and 24 and a supporting βG–βH loop are removed.

The importance of loop I for the proper functioning of the enzyme is underscored by its relatively high number of strictly conserved residues and its appearance in pro- and eukaryotic species. A survey of the currently available DHFR amino acid sequences, excluding those that are plasmid-derived, shows that of the 159 residues in *E. coli* DHFR, only 10 are strictly conserved in all bacterial and vertebrate DHFRs. Four of these strictly conserved residues are found in loop I at positions that flank the central hairpin turn. Among the strictly conserved residues, Ile14 has been shown (Bystroff et al., 1990) to form a hydrogen bond between its backbone oxygen atom and N7 nitrogen of the nicotinamide carboxamide moiety of $NADP^+$; however, this occurs only in the E·$NADP^+$·folate ternary complex. The side chain of another strictly conserved residue, Trp22, interacts hydrophobically with the 2-amino-4-oxopyrimidine moiety of folate and takes part in the formation of a network of hydrogen bonds that involves a fixed water molecule, the O4 oxygen of folate, and the carboxyl group of Asp27, which is the only ionizable residue in the active site and is required for proper catalysis (Howell et al., 1986). This suggests that an important role of loop I is stabilizing the transition state and aligning the substrates for optimal hydride transfer, if one assumes that similar protein conformational changes take place in the E·$NADP^+$·H_2F ternary complex.

In order to obtain insights into the functional role of the highly mobile loop of the active site, we constructed a mutant *E. coli* DHFR, DL1, in which the four residues that form the central hairpin of loop I were deleted and the gap was filled with a glycine residue. We have previously utilized a similar approach to manipulate other elements of secondary structure (Li & Benkovic, 1991). For the DL1 mutant, a number of enzymatic properties, including substrate binding and catalysis, were analyzed and compared to wild-type DHFR. Some of the dynamic properties of the DL1 mutant, particularly in the loop I region, were investigated using two-dimensional ^1H NMR methods and also compared to the wild-type protein.

MATERIALS AND METHODS

Materials

Dihydrofolate was prepared by the reduction of folate by using the method of Blakley (1960). (6*S*)-Tetrahydrofolate was prepared by using *E. coli* dihydrofolate reductase to reduce H_2F and purified on DE-52 resin by eluting with a trimethylammonium bicarbonate linear gradient (Curthoys et al., 1972). [4′(*R*)-^{2}H]NADPH was prepared by using *Leuconostoc mesenteroides* alcohol dehydrogenase (Stone & Morrison, 1982) obtained from Research Plus Inc. and then purified by the method of Viola et al. (1979). The concentrations of the substrates were determined as described (Fierke et al., 1987). Methotrexate (MTX) was purchased from Sigma, and its concentration was determined spectrophotometrically in 0.1 M NaOH [ϵ_{302} = 22 100 M^{-1} cm^{-1}] (Seeger et al., 1949).

The plasmid pTZWT1-3 which carries the *E. coli* DHFR gene (*fol*), an overexpression promoter (Iwakura & Tanaka, 1992), and renders ampicillin resistance, was generously provided by Drs. M. Iwakura and C. R. Matthews in our department. Oligonucleotides for mutagenesis were prepared by American Synthesis Inc. Endonucleases were purchased from New England Biolabs, and T_4 DNA ligase was from IBI.

Methods

Cassette-Directed Mutagenesis. Two unique restriction endonuclease sites, *Nhe*I and *Nco*I, are available in the *fol* gene cloned in plasmid pTZWT1-3 (Iwakura and Matthews, unpublished results) at positions that flank the codons encoding the central section of loop I of the *E. coli* DHFR. In order to delete residues Met16-Glu17-Asn18-Ala19 from the wild-type enzyme and insert a glycine residue after Gly15 (see Table I), pTZWT1-3 plasmid DNA was subjected to *Nhe*I and *Nco*I digestion. The larger DNA fragment was isolated by using agarose gel electrophoresis and an oligonucleotide purification cartridge (Applied Systems). The fragment DNA was ligated, using T_4 DNA ligase, to a double-stranded DNA obtained by annealing two synthetic oligonucleotides, 5′-CTAGCGGTAG ATCGCGTTAT CGGCGGCATG C-3′ and 5′-CATGGCATGC CGCCGATAAC GCGATCTACC G-3′. The annealed double-stranded DNA has sticky ends compatible to those generated by *Nhe*I and *Nco*I digestion. The ligation product was used to transform *E. coli* (strain DH5αF′IQ) cells. The desired mutant plasmid was selected by the presence of a newly introduced *Sph*I restriction site (underlined) and confirmed by complete sequencing of the gene (Sanger, 1981). The mutant plasmid was designated as pLLa6-2.

Enzyme Purification. Plasmid pLLa6-2 was used to transform *E. coli* cells (strain MK30-3) for the expression of DL1 DHFR. The mutant enzyme was purified, essentially as described (Chen et al., 1987), by using an MTX affinity resin. The enzyme was eluted from the MTX resin with borate buffer (pH 9.0) containing 0.5 mM folate. After dialysis into Tris-HCl buffer (pH 7.2), the enzyme was then separated from folate and bound nucleotides by passage through a DEAE-Sephacel column. The enzyme concentrations were determined by MTX titration (Williams et al., 1979).

Kinetic Measurements. Unless otherwise noted, all kinetic and equilibrium measurements were conducted at 25 °C in a buffer that contained 50 mM 2-(*N*-morpholino)ethanesulfonic acid, 25 mM Tris, 25 mM ethanolamine, and 100 mM NaCl (MTEN buffer, pH 5–10). The ionic strength of this

buffer remains constant over the pH range used (Ellis & Morrison, 1982). For the determination of the steady-state kinetic parameters, the enzyme (1.2 nM) was preincubated with either 60 μM NADPH or 20 μM H_2F for 2–3 min. The reaction was monitored spectrophotometrically at 340 nm (ϵ = 11 800 M^{-1} cm^{-1}; Stone & Morrison, 1982), and the data were fitted to eq 1, where v is the initial velocity and S is the substrate

$$v = VS/(K_M + S) \quad (1)$$

concentration, by a nonlinear regression method to yield the maximum velocity (V) and the Michaelis constant (K_M). Increasing concentrations of the substrate or cofactor were used until no significant increase of the initial reaction rate was observed. Deuterium isotope effects on the reaction rate (^DV) were determined by using [4'(R)-^{2}H]NADPH. Pre-steady-state data were obtained by monitoring the enzyme fluorescence quenching or the absorbance change during turnover as described (Fierke et al., 1987; Dunn & King, 1980; Cayley et al., 1981) using a stopped-flow spectrophotometer (Applied Photophysics, Leatherhead, England). For the determination of dissociation rate constants by competition stopped-flow (Table III), the enzyme (2–6 μM) was incubated for 2–3 min with H_4F (15 μM) and a saturating amount of the ligand as indicated. The mixture was then mixed with an equal volume of a solution of H_4F (15 μM), and the trapping ligand was in excess. Changes in the intrinsic fluorescence of the enzyme (excitation 290 nm, emission 340 nm), or in the fluorescence energy transfer of enzyme-bound NADPH (excitation 290 nm, emission 450 nm), were monitored. The data were fitted with a simple exponential decay. For the determination of binding rate constants by relaxation stopped-flow (Table IV), the enzyme solution (2–6 μM) was mixed with an equal volume of NADPH solutions of increasing concentrations (typically 1–50 μM). The observed rate constants (k_{obs}) of fluorescence quenching were fitted to $k_{obs} = k_{on}[L] + k_{off}$ (data not shown). Equilibrium dissociation constants were measured using fluorescence quenching as described (Stone & Morrison, 1982) by following the quenching of the intrinsic enzyme fluorescence as a function of added ligand concentration. The steady-state turnover rate constant (k_{cat}) is obtained by dividing V by the total enzyme concentration used. The k_{HYD}–pH profile was fitted to eq 2 where k_{obs} is the hydride-transfer rate observed at each pH value, k_{HYD} is the pH-independent parameter, K_a is an acid dissociation constant, and H is [H^+].

$$k_{obs} = k_{HYD}/(1 + K_a/H) \quad (2)$$

NMR Analysis. Sample preparation has been previously described (Falzone et al., 1990). Wild-type DHFR was purified as described above. NOESY and CAMELSPIN (ROESY) experiments were acquired using standard methods at 500 MHz (Kumar et al., 1980; Bothner-By et al., 1984). The mixing time for ROESY experiments was 40 ms with a field strength of 2.5 kHz for spin locking. NOESY mixing times were from 10 to 75 ms. The spectral width was 12 500 Hz, and 8K data complex points were collected. The ω_1 spectral width was 6097 Hz, and between 420 and 512 experiments were acquired. The data were then zero-filled to 1024 real points. All spectra were acquired with sine modulation in the t_1 dimension (Otting et al., 1986). Sample temperature was maintained at 298 K, and spectra were referenced to H_2O at 4.76 ppm.

Partial ^{1}H NMR assignments for the wild-type–folate complex have been reported (Falzone et al., 1990). Owing to the complexity of the ^{1}H spectra for apo wild-type DHFR, only a limited number of assignments are reported here. More extensive assignments for the DL1 apoprotein will be presented elsewhere. Assignments pertinent to this paper are discussed in the text.

Table I: Primary Structures of Loop I in Wild-Type DHFR (Residues 9–24) and the DL1 Mutant[a]

enzyme	amino acid sequence
E. coli[b]	AVDRVIGMENAMPWNL
DL1	AVDRVIGG-------MPWNL

[a] The underlined residues form hairpin turns in the ternary complex (Bystroff et al., 1990). [b] Volz et al. (1982).

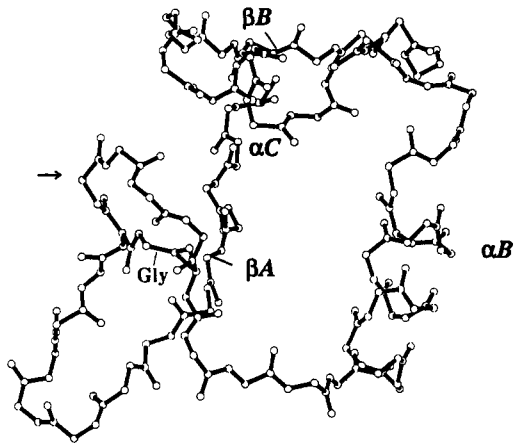

FIGURE 1: Superimposed backbones of the *E. coli* DHFR (residues 1–54) and the DL1 mutant enzyme. Computer graphic modeling based on the structure of the E·MTX complex of the *E. coli* enzyme suggests that it is possible to replace residues Met16 to Ala19 (arrow) with a glycine without causing major structural perturbations.

RESULTS

Deletion of the Middle Section of Loop I. The amino acid sequences of loop I in *E. coli* DHFR and the DL1 mutant enzyme are given in Table I. There are two hairpin turns in loop I: one at the beginning (residues 9–12, Ala-Val-Asp-Arg) and the other in the central part of the loop (residues 16–19, Met-Glu-Asn-Ala). This central hairpin turn is formed only in the E·$NADP^+$·folate ternary complex (Bystroff et al., 1990), and presumably also in the E·NH·H_2F ternary complex though no structural data are available for this latter complex. In other complexes and in the apoenzyme, the active-site cavity is more exposed to solvent. Residues 16–19 in the E·MTX binary complex assume an ordered conformation, but it is different from that observed in the ternary complex with Met20 now pointing away from the active site (Bolin et al., 1982; Bystroff & Kraut, 1991). In the structure of the E·MTX complex, the distance between the carbonyl carbon of Met16 and the amino nitrogen of Ala19 is similar to the length of an amino acid residue in a peptide chain (3.8 Å). This suggests that it is possible to delete residues 16–19, and fill the resulting gap with a glycine and cause only local conformational changes (Figure 1).

Steady-State Kinetics. The steady-state kinetic parameters are given in Table II. The turnover rate constant (k_{cat}) of the mutant enzyme catalyzed reaction is 0.7 s^{-1} at pH 6, markedly lower than the wild-type value. The deuterium isotope effect on the reaction rate indicates that the rate-limiting step is not product release, as is observed for the wild-type mechanism, but is the rate of hydride transfer.

The changes in the Michaelis constant (K_M) for either H_2F or NADPH are only marginal. The K_M values, unlike those exhibited by the wild-type enzyme, are similar to their

Table II: Kinetic Parameters Associated with the DL1 Mutant DHFR-Catalyzed Reaction (pH 6.0)

	DL1	*E. coli*[a]
k_{cat} (s^{-1})	0.7 ± 0.1	12
^{D}V	2.5 ± 0.2	1
K_M (H_2F, μM)	2.0 ± 0.2	0.7
K_D (H_2F, μM)	1.7 ± 0.2	0.22
K_M (NADPH, μM)	5.3 ± 1.2	5.0
K_D (NADPH, μM)	3.1 ± 0.2	0.33

[a] Fierke et al. (1987).

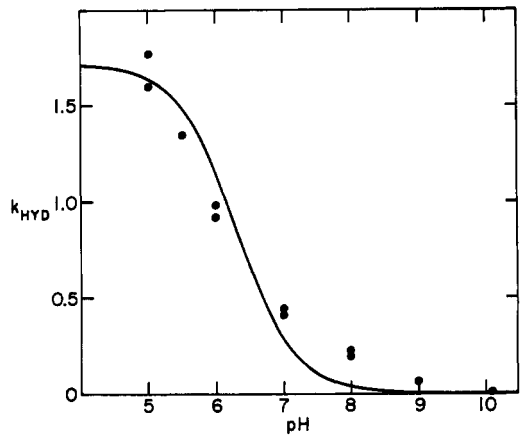

FIGURE 2: Observed hydride-transfer rate as a function of pH for the DL1 mutant DHFR determined using stopped-flow techniques. The enzyme (2.2–11.2 μM) was preincubated with NADPH (116 μM) and then mixed with H_2F (53–105 μM). The change in absorbance was monitored at 340 nm. The data were fitted to eq 2 (see Methods) by nonlinear regression ($R^2 = 0.98$). The pH-independent k_{HYD} is 1.7 ± 0.1 s^{-1}, and the pK_a is 6.2 ± 0.1.

Scheme I

$$E{\cdot}NH + H_2F \underset{K_D}{\rightleftharpoons} E{\cdot}NH{\cdot}H_2F \overset{k_{hyd}}{\rightleftharpoons} E{\cdot}N{\cdot}H_4F \overset{fast}{\rightleftharpoons} E{\cdot}NH{\cdot}H_4F \overset{k_{off}}{\rightleftharpoons} E{\cdot}NH + H_4F$$

respective equilibrium dissociation constants (K_D). This arises from a kinetic pathway that follows a simple Michaelis mechanism in which the binding of substrate is followed by a rate-determining chemical step. A simplified kinetic pathway of the *E. coli* DHFR-catalyzed reaction applicable to DL1 may be represented by Scheme I. The relationship between K_M and K_D can be described by eq 3 where k_{HYD} and

$$K_M = K_D \frac{k_{off}}{k_{off} + k_{HYD}} \quad (3)$$

k_{off} are the hydride-transfer rate constant and the dissociation rate constant for H_4F, respectively (see below). If k_{HYD} is much less than k_{off}, K_M and K_D are similar, as observed for the DL1 mutant enzyme catalyzed reaction. For the wild-type enzyme, the relationship between K_M and K_D is more complicated and cannot be accounted for by Scheme I.

Hydride Transfer. The deletion of residues 16–19 markedly impairs the hydride-transfer process. This is evident from stopped-flow experiments in which the hydride-transfer reaction was monitored over a range of pH values (Figure 2). The pH-independent hydride-transfer rate (k_{HYD}) for the DL1 mutant enzyme catalyzed reaction is 1.7 ± 0.1 s^{-1}, which represents a dramatic decline from k_{HYD} = 950 s^{-1} observed for wild-type *E. coli* DHFR. A full deuterium isotope effect of 3.1 ($^{D}k_{HYD}$) on k_{HYD} was observed, and the hydride-transfer rate was 0.95 s^{-1} measured at pH 6. By using the relationship derived from Scheme I, $1/k_{cat} = 1/k_{HYD} + 1/k_{off}$, where k_{off} is the off rate (Table III) for H_4F release, the calculated k_{cat} at pH 6 is 0.87 s^{-1}, which is in satisfactory agreement with the steady-state turnover rate of 0.7 s^{-1} measured at the same pH. The pK_a value obtained from the k_{HYD}–pH profile is 6.2, which represents the ionization constant of the Asp27 residue in the E·NH·H_2F ternary complex. This value is similar to that observed for the wild-type enzyme (pK_a = 6.5; Fierke et al., 1987). This nearly unchanged pK_a indicates that the environment of Asp27 in the mutant enzyme closely resembles that in the wild-type enzyme.

Table III: Pre-Steady-State Kinetic Parameters Associated with the DL1 Mutant DHFR-Catalyzed Reaction (pH 6.0)

			k_{off} (s^{-1})	
ligand	enzyme species	trapping ligand	mutant	*E. coli*[a]
H_4F	E·H_4F	MTX	8.1 ± 0.7	1.4
H_4F	E·NH·H_4F	MTX	10.3 ± 1.2	12
H_4F	E·N·H_4F	MTX	5.2 ± 0.7	2.4
N	E·N·H_4F	NH	437 ● 5	200

[a] Fierke et al. (1987).

Table IV: Kinetic Rate Constants Associated with Cofactor Binding (NADPH) for the DL1 Mutant and Wild-Type DHFR, pH 6.0

	DL1	wild type (*E. coli*)[a]
k_{on} (μM^{-1} s^{-1})	44.1 ± 5.5	20
k_{off} (s^{-1})	185 ± 33	3.5
k_{off}/k_{on} (μM)	4.2 ± 0.9	0.18
K_D (μM)	3.1 ± 0.2	0.33

[a] Fierke et al. (1987).

The rate of the reverse reaction (k_{rev} for the net conversion of H_4F and $NADP^+$ to form H_2F and NADPH) was determined from the increase in absorbance at 340 nm by using stopped-flow techniques; it was found to be 0.073 ± 0.002 s^{-1} at pH 9.0. This value was virtually constant with H_4F concentrations varying from 0.3 to 0.6 mM and $NADP^+$ concentrations from 1.25 to 2.5 mM. Compared with the wild-type value of 0.48 s^{-1} obtained under similar conditions (Fierke et al., 1987), the reverse reaction rate is decreased by about 10-fold. The internal equilibrium constant ($K_{int} = k_{HYD}/k_{rev}$) of the DL1 mutant enzyme catalyzed hydride-transfer step was estimated to be about 10 at pH 7, with k_{HYD} being 0.5 s^{-1} at this pH value. The wild-type K_{int} value at the same pH is about 500, estimated by using a k_{HYD} value of 250 s^{-1} determined at pH 7 (Fierke et al., 1987).

Release of H_4F from Various Enzyme–Ligand Complexes. A characteristic of the *E. coli* DHFR-catalyzed reaction is the synergism in product release. That is, the off rate of H_4F is significantly elevated by the binding of NADPH to the E·H_4F binary complex following the release of $NADP^+$ (Fierke et al., 1987). The k_{off} values for the release of H_4F from various complexes of the mutant enzyme were determined by a stopped-flow competition method and are given in Table III. The off-rate constant for H_4F in the E·NH·H_4F complex is similar to the wild-type value; however, the off-rate constants for H_4F in the other two complexes of the kinetic pathway, E·H_4F and E·N·H_4F, are increased by severalfold. Thus, there is little enhancement of the product off rate by cofactor binding. It is plausible that the conformational changes associated with the movement of loop I are an important factor in the binding synergism exhibited by the wild-type enzyme which is now absent in the deletion mutant.

Ligand Binding. The kinetic binding rate constants for the interaction of NADPH with the DL1 mutant enzyme were determined by using the stopped-flow relaxation method. The results are given in Table IV. Compared with the wild-type values, the most significant change in the binding of NADPH

Scheme II

$$\begin{array}{ccccc} E_1 & + & NH & \rightleftharpoons & E_1 \cdot NH \\ \updownarrow & & & & \updownarrow \\ E_2 & + & NH & \rightleftharpoons & E_2 \cdot NH \end{array}$$

is the k_{off} value, which is increased by about 50-fold. The dissociation constant for the initial binding of NADPH, calculated from k_{off}/k_{on}, is increased accordingly, and becomes comparable with the measured equilibrium dissociation constant, K_D.

Absence of a Slow Fluorescent Phase. It has been shown that *E. coli* DHFR possesses two conformers in solution, known as E_1 and E_2, with an equilibrium constant ($K_{eq} = E_1/E_2$) close to 1 (Cayley et al., 1981). The cofactor NADPH can bind to both conformers, although the affinities are very different as shown in Scheme II (Adams et al., 1989; $k_{off}/k_{on} = 0.15\ \mu M$ for E_1 and $k_{off}'/k_{on}' = 14\ \mu M$ for E_2). The binding of NADPH causes a slow, ligand-independent, conversion of the conformers at a rate of $0.032\ s^{-1}$ toward the tighter binding form, and 99% of the enzyme exists as E_1·NADPH at equilibrium. Owing to the slow interconversion between these two conformers, exchange cross-peaks have not been observed at room temperature in the spectra of the wild-type apoprotein or in the MTX complex (where both conformers are present) for this equilibrium process (Falzone et al., 1991).

For the DL1 enzyme, the slow, ligand-independent, phase in the quenching of intrinsic enzyme fluorescence (data not shown) is absent. Also, the NMR spectra of the DL1 apoprotein show an absence of a second form. These data indicate that the mutant enzyme exists in solution as one of these conformers. The active site of DL1 may now have adopted conformational elements which are similar to the wild-type conformer that has the lower affinity for NADPH, namely, E_2. It has been reported (Adams et al., 1991) that there is a predominant species similar to E_2 for several mutant DHFR enzymes; however, unlike the DL1 mutant, these species undergo E_2 to E_1 conversion in the presence of ligand at a rate similar to that exhibited by the wild-type enzyme, as indicated by a substantial slow, ligand-independent phase observed during fluorescence quenching.

Evidence for a Two-Site Exchange in Loop I of the Wild-Type Apoprotein. In the wild-type apoprotein, there is an exchange process which is slow on the NMR time scale at room temperature (298 K) that is detected in ROESY or NOESY experiments. Figure 3A shows a region of a 40-ms ROESY spectrum of apo wild-type DHFR where only the diagonal and exchange cross-peaks are plotted. It clearly shows exchange cross-peaks. Corresponding cross-peaks in similar experiments that arise from protein resonances have not been detected at room temperature in the binary folate or MTX complexes (Falzone et al., 1990, 1991). The same spectral region is shown in Figure 3B for the DL1 apoprotein. Exchange cross-peaks are now absent, and we conclude that deletion of the central hairpin turn forming residues in loop I affects the observed wild-type exchange process. Several interpretations are possible: the process could be too slow to observe exchange cross-peaks, the exchange may have been eliminated, or the conformational exchange is now fast on the NMR time scale and average resonances are observed.

Several of the exchanging resonances shown in Figure 3A can be tentatively assigned to residues which are proximal to the Met20 loop. For example, the cross-peaks at 0.16 and 0.23 ppm result from the exchange of a $C^{\delta}H_3$ of Leu24; Leu24 shows NOEs to the $C^{\delta}H$ of Trp22. The $C^{\gamma}H_3$ of Ile115 is found at 0.09 and 0.15 ppm and is also in dipolar contact with

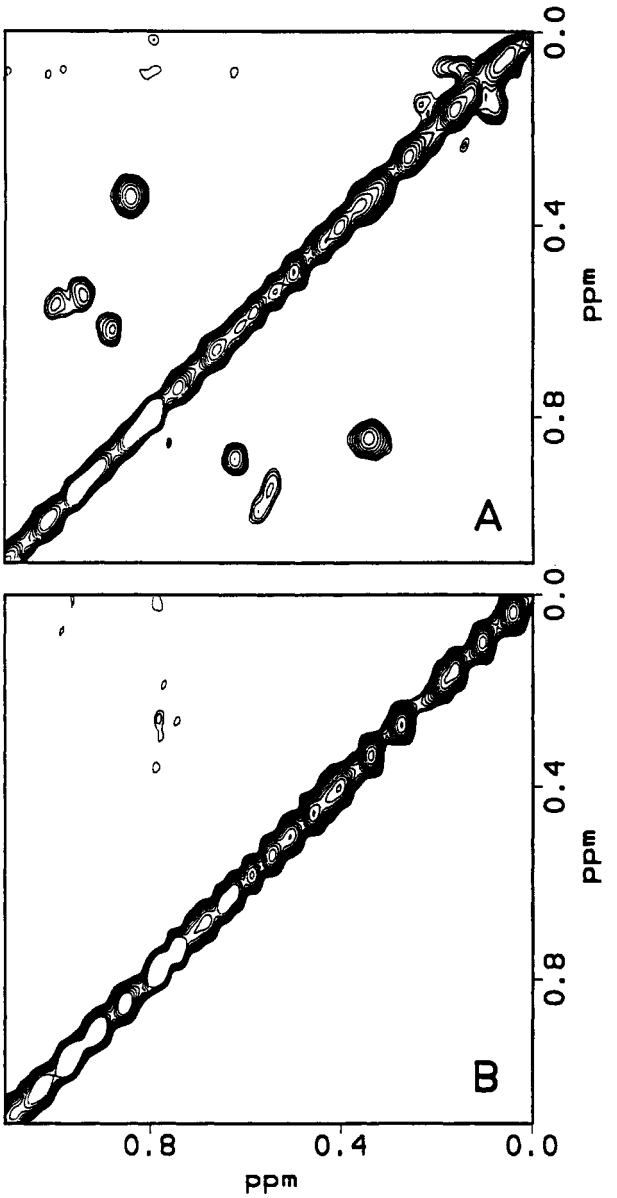

FIGURE 3: (A) Region of a 40-ms ROESY spectrum for apo wild-type DHFR. Only the diagonal and exchange cross-peaks are plotted (negative levels). Note the abundance of exchange cross-peaks that are slow on the NMR time scale. (B) The same region as in (A) for a 40-ms ROESY experiment on apo-DL1 DHFR. No exchange cross-peaks can be detected under these conditions.

Trp22. Additionally, the $C^{\delta}H_3$ of Ile115 is found in two environments at –0.67 and –0.87 ppm (data not shown). The other exchange cross-peaks found in Figure 3A may arise from proximal aliphatic side-chain protons (such as Ala7, Ala9, Met16, Ala19, Met20, Pro21, Ala117, and Val119), but they cannot be unambiguously assigned at this time.

The $N^{\epsilon}H$ of Trp22 can be assigned in the apoprotein and is also found to exchange between two environments at 298 K. (The assignment of these protons is based on NOEs between $N^{\epsilon}H$ and the protein matrix. The observed NOE pattern is similar to others previously studied.) Resolved saturation-transfer cross-peaks are found between the two $N^{\epsilon}H$ resonances at 298 K in the downfield region of NOESY or ROESY spectra of the wild-type apoprotein. These exchange cross-peaks can even be observed at mixing times as short as 10 ms (Figure 4A). More intense cross-peaks are observed in longer mixing time experiments until relaxation effects dominate (at about 50 ms). A plot of the same regions as Figure 4A (wild-type apoprotein) is presented in Figure 4B

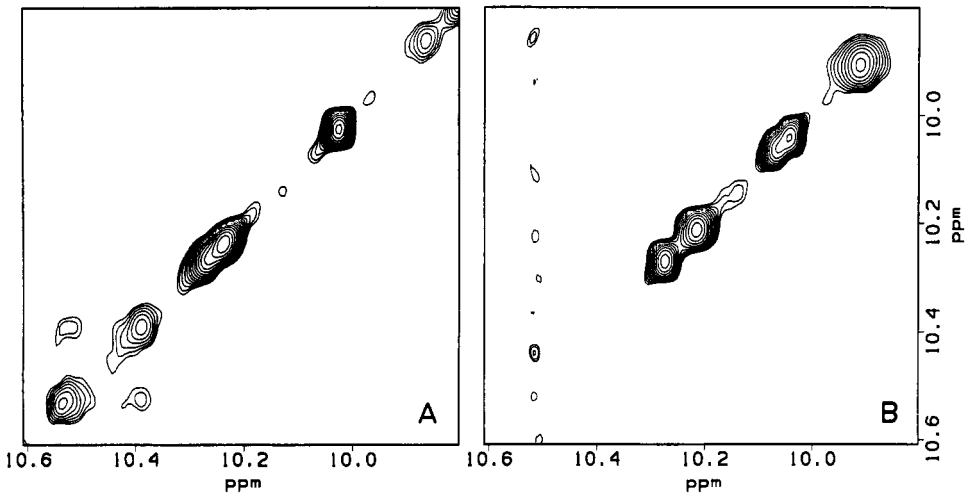

FIGURE 4: (A) Most downfield region of a 10-ms NOESY experiment on apo wild-type DHFR. This mixing time was chosen because the exchange of $N^{\epsilon}H$ of Trp22 between two environments can be detected while most NOEs are still weak. This exchange is also observed in a 40-ms ROESY spectrum. (B) The same region of a 10-ms NOESY experiment for the apo-DL1 mutant protein showing the absence of the exchange cross-peaks. The $N^{\epsilon}H$ is now at 10.04 ppm for this enzyme.

(DL1 apoprotein). In this 10-ms NOESY spectrum of DL1 apoprotein, the saturation-transfer cross-peaks detected previously are now absent, suggesting that most of the intrinsic flexibility in this loop has been removed by deletion of the residues that form the hairpin turn in the ternary complex. Exchange cross-peaks cannot be detected in longer mixing time NOESY or ROESY spectra of the DL1 mutant. An analysis of the buildup curve for the wild-type protein is in progress.

NOEs are observed from Met20 to Trp22 in the DL1 apoprotein; specifically, these are between $C^{\epsilon}H_3$ of Met20 and $C^{\delta}H$, $N^{\epsilon}H$, and $C^{\zeta 2}H$ of Trp22 as detected in a 75-ms NOESY. Met20 has not been assigned in wild-type apoprotein spectra which perhaps stems from the observed exchange process. The $C^{\epsilon}H_3$ of Met20 can be assigned in the spectra of the wild-type folate complex and shows NOEs to $C^{\zeta 1}H$, $C^{\eta}H$, and $C^{\zeta 3}H$ of Trp22, indicating a similar, but not identical, arrangement of side chains in the loop I region. Since NOEs are readily detected between Met20 and Trp22 when the wild-type protein has folate bound in the active site, the ability to detect similar NOEs in the DL1 apoprotein suggests that the Met20 loop is now in a restricted conformation. The X-ray crystal structures also show an ordered Met20 loop when the folate site is occupied in the wild-type protein (Bystroff & Kraut, 1991).

DISCUSSION

The removal of the hairpin-forming residues from the central part of loop I imposes small perturbations on the ground-state binding of both NADPH and H_2F with its greatest impact seen on the rate of hydride transfer. The K_D values for the cofactor and the substrate are each increased by about 10-fold, reflecting in the absence of the loop a destabilization of the corresponding binary and ternary complexes by about 1.4 kcal/mol. In contrast, k_{HYD} for the deletion mutant declines from 950 to 1.7 s^{-1}. From the data in Table II, the values for k_{hyd}, k_{rev}, and the internal equilibrium constants for DL1 and wild-type enzymes, one can calculate the $\Delta\Delta G^{\circ\ddagger}$ for the process of $E + NH + H_2F \rightarrow (E{\cdot}NH{\cdot}H_2F)^{\ddagger}$ (Table V). We assume the free enzymes are equal in free energy ($\Delta\Delta G^{\circ} = 0$). This analysis reveals that the loop stabilizes the transition state involving hydride transfer by about 6.2 kcal/mol relative to the free enzymes, corresponding to a factor of ca. 3.5×10^4 for this process relative to wild-type enzyme. Thus, one of the primary functions of the newly formed hairpin turn is to properly align the nicotinamide and pteridine rings in the active site (a form of transition-state stabilization).

Table V: Comparison of the Standard Free Energy Differences for the Equilibrium Association and the Hydride-Transfer Step between the DL1 Mutant and Wild-Type Enzyme

process	$\Delta\Delta G^{\circ}$ (DL1-WT, kcal)[a]
$E + NH \rightleftharpoons E{\cdot}NH$	1.3
$E{\cdot}NH + H_2F \rightleftharpoons E{\cdot}NH{\cdot}H_2F$[b]	1.2
$E{\cdot}NH{\cdot}H_2F \rightarrow E{\cdot}N{\cdot}H_4F$	3.7
$E{\cdot}N{\cdot}H_4F \cdot \rightarrow E{\cdot}NH{\cdot}H_2F$	1.9
$E{\cdot}NH{\cdot}H_2F \rightleftharpoons E{\cdot}N{\cdot}H_4F$[c]	−2.6
$E + NH + H_2F \rightarrow (E{\cdot}NH{\cdot}H_2F)^{\ddagger}$	6.2[d]

[a] $\Delta\Delta G^{\circ}$ was calculated using the relationship: $\Delta\Delta G^{\circ} = -RT \ln [K_D(DL1)/K_D(wt)]$. The standard free energy for the hydride-transfer process was calculated using $\Delta G^{\circ} = -RT [\ln (kT/h) - \ln (k_{hyd})]$, and $\Delta\Delta G^{\circ}$ is given by $\Delta G^{\circ}(DL1) - \Delta G^{\circ}(wt)$. Reaction conditions are given under Materials and Methods. [b] Assumes binding of H_2F to E·NH is given by K_D (H_2F); see Table II. [c] Calculated using the pH-independent values. [d] Calculated from the sequence $E + NH + H_2F \rightleftharpoons E{\cdot}NH{\cdot}H_2F$ (1.3 + 1.2 kcal) plus $E{\cdot}NH{\cdot}H_2F \rightarrow E{\cdot}N{\cdot}H_4F$ (3.7 kcal).

Crystallographic data on the folate–$NADP^+$ ternary complex (Bystroff et al., 1990; Bystroff & Kraut, 1991) provide some evidence for the importance of these residues in the reactive complex. Forming the hairpin turn with residues 16–19 imports Ile14 and Met20 to the active site. The backbone carbonyl oxygen of Ile14 forms a new hydrogen bond with the N7 nitrogen of nicotinamide and interacts with the C2 carbon of the same moiety through dipole–dipole interactions while the side chains of Ile14 and Met20 establish hydrophobic interactions with the nicotinamide ring. In the folate binding site, the side chain of Trp22 interacts hydrophobically with the 2-amino-4-oxopyrimidine moiety of the substrate. In addition, Trp22 is among the few residues that are involved in a network of hydrogen bonds by fixed water molecules and Asp27, the only ionizable residue in the active site. These interactions may be disrupted in the DL1 enzyme.

Two-dimensional NMR spectroscopy provides evidence for small structural perturbations near the site of the deletion. Previously detected NOEs between assigned residues form a similar pattern to binary wild-type complexes. In particular, NOEs between $C^{\delta}H$, $N^{\epsilon}H$, and $C^{\zeta 2}H$ of Trp22 and $C^{\epsilon}H_3$ of Met20 are observed in the DL1 protein and suggest a slight conformational change between this mutant apoprotein and the binary folate complex. In the folate complex, NOEs were

observed between the $C^{\epsilon}H_3$ of Met20 and $C^{\beta 2}H$, $C^{\gamma}H$, and $C^{\beta 3}H$ of Trp22. With the deletion of residues 16–19, the main effect may be a reduction in the flexibility of this mobile loop which is consistent with the ability to observe NOEs between Met20 and Trp22. The exchange process observed for the wild-type apoprotein is no longer detected in the DL1 mutant. Either the deletion has removed (or slowed) the exchange process or it has lowered the activation barrier and the frequency of exchange is now too fast to observe resolved resonances.

A consequence of the apparent flexibility of the middle section of loop I in the wild-type apoenzyme is that it generates an opening of the active site to solvent and cofactor (Bystroff & Kraut, 1991). NADPH binds to the enzyme in an extended conformation with its nicotinamide ring positioned at the opening near loop I. Bystroff et al. (1990) reported that the central part of loop I remains disordered in the $NADP^+$ binary complex; however, the crystals of the NADPH binary complex are isomorphous with the folate–$NADP^+$ ternary complex in which the central part of loop I is now ordered. These authors asserted that, assuming that isomorphous crystals have similar protein conformations, the reduced nicotinamide mononucleotide (NMN) moiety of NADPH in the NADPH binary complex is ordered and binds in the same way as the oxidized NMN of $NADP^+$ in the folate–$NADP^+$ ternary complex. This is consistent with an earlier observation by ^{31}P NMR that a broad resonance for the 5′-phosphate suggested a loosely bound NMN of $NADP^+$ whereas the reduced NMN of NADPH is more ordered as shown by a sharp ^{31}P signal (Cayley et al., 1980).

These structural data enable us to envision the role of the conformational changes involving the middle section of loop I. An accessible active site is present in the apoprotein as evidenced by the disordered middle portion of loop I by X-ray crystallography and by the slow exchange observed in the ^1H NMR spectra for resonance associated with residues proximal to the loop in the wild-type protein. Upon binding of cofactor, a hairpin turn forms in the loop and folds over the NMN moiety, and a hydrogen bond is made across the gap between the side chain of Asn18 in loop I and the backbone carbonyl oxygen of His45 in the αC-helix. Thus, the middle section of loop I serves as a gate to the active center. The kinetic binding rate constant determined by stopped-flow techniques for the binding of NADPH (Table IV) is consistent with this view. The on rate observed for the mutant enzyme is comparable to the wild-type value, indicating similar accessibility to the cofactor binding site. However, the off rate for NADPH becomes much faster (185 vs 3.5 s^{-1}) in the mutant enzyme. The off rate for H_4F likewise is increased but to a lesser extent (8.1 vs 1.4 s^{-1}) so that the effect of binding of NADPH on the dissociation of H_4F is much less pronounced (approximately a factor of 1.2 vs 9, Table III). These phenomena may reflect a more open active site in the absence of the hairpin turn or may also be due to the inability of the mutant enzyme, lacking the hairpin-forming residues, to recruit additional side chains for binding cofactor. The finding of only one complex in the binding of cofactor, however, cannot be viewed as evidence for the proximity of the loop region to the origin of the isomerization since mutations at Tyr100 drastically shift the E_1/E_2 equilibrium in favor of E_2 (Adams et al., 1991).

A mobile or flexible loop may provide the best structural motif for performing tasks that require extensive conformational modifications. Our findings are consistent with the view that, when an active-site cavity of an enzyme is composed of mobile structural elements and other less flexible secondary structures, the latter would contribute primarily to ground-state binding of the substrate, while the former would contribute more to the transition-state stabilization, which often requires "tightening-up" of the active center as a result of substrate-induced conformational changes. In this example, the side chain of Met20 is introduced for this purpose.

Flexible loops provide enzymes with an induced-fit mechanism for substrate binding; DHFR has exploited this motif to its catalytic advantage. It has been pointed out (Herschlag, 1988) that an "induced-fit" improves substrate specificity; a highly mobile loop, such as loop I in DHFR, serves such a purpose by allowing access of substrates to the active site and then encapsulating the reactive complex through a conformational change. This mechanism not only would bring about additional intrinsic binding energy to enhance catalysis but also would permit a "fine-tuning" of the catalytic mechanism of the enzyme by way of mutation. The DL1 mutant shows that the inability to utilize the residues in loop I has a detrimental and specific effect on enzyme catalysis. Clearly, a loop represents an ingenious solution by this and other enzymes to a particular catalytic problem.

ACKNOWLEDGMENT

We thank Drs. M. Iwakura and C. R. Matthews for furnishing plasmid pTZWT1-3.

REFERENCES

Adams, J., Johnson, K., Matthews, R., & Benkovic, S. J. (1989) *Biochemistry 28*, 6611–6618.

Adams, J. A., Fierke, C. A., & Benkovic, S. J. (1991) *Biochemistry 30*, 11046–11054.

Barford, D., & Johnson, L. N. (1989) *Nature 340*, 609–616.

Blakley, R. L. (1960) *Nature (London) 188*, 231–232.

Bolin, J. T., Filman, D. J., Matthews, D. A., Hamlin, R. C., & Kraut, J. (1982) *J. Biol. Chem. 257*, 13650–13662.

Bothner-By, A. A., Stephens, R. L., Lee, J., Warren, C. D., & Jeanloz, R. W. (1984) *J. Am. Chem. Soc. 106*, 811–813.

Bystroff, C., & Kraut, J. (1991) *Biochemistry 30*, 2227–2239.

Bystroff, C., Oatley, S. J., & Kraut, J. (1990) *Biochemistry 29*, 3263–3277.

Cayley, P. J., Feeney, J., & Kimber, B. J. (1980) *Int. J. Biol. Macromol. 2*, 251–255.

Cayley, P. J., Dunn, S. M. J., & King, R. W. (1981) *Biochemistry 20*, 874–879.

Chen, J.-T., Taira, K., Tu, C.-P. D., & Benkovic, S. J. (1987) *Biochemistry 26*, 4093–4100.

Curthoys, H. P., Scott, J. M., & Rabinowitz, J. C. (1972) *J. Biol. Chem. 247*, 1959–1964.

Dunn, S. M. J., & King, R. W. (1980) *Biochemistry 19*, 766–773.

Ellis, K. J., & Morrison, J. F. (1982) *Methods Enzymol. 87*, 405–426.

Falzone, C. J., Benkovic, S. J., & Wright, P. E. (1990) *Biochemistry 29*, 9667–9677.

Falzone, C. J., Wright, P. E., & Benkovic, S. J. (1991) *Biochemistry 30*, 2184–2191.

Fetrow, J. S., Cardillo, T. S., & Sherman, F. (1989) *Proteins: Struct., Fund., Genet. 6*, 372–381.

Fierke, C. A., Johnson, K. A., & Benkovic, S. J. (1987) *Biochemistry 26*, 4085–4092.

Herschlag, D. (1988) *Bioorg. Chem. 16*, 62–96.

Howell, E. E., Villafranca, J. E., Warren, M. S., Oatley, S. J., & Kraut, J. (1986) *Science (Washington, D.C.) 231*, 1123–1128.

Iwakura, M., & Tanaka, T. (1992) *J. Biochem. (Tokyo)* (in press).

Kuipers, O. P., Thunnissen, M. M. G. M., de Geus, P., Dijkstra, B. W., Drenth, J., Verheij, H. M., & de Haas, G. H. (1989) *Science (Washington, D.C.) 244*, 82–85.

Kumar, A., Ernst, R. R., & Wüthrich, K. (1980) *Biochem. Biophys. Res. Commun. 95*, 1–6.

Leszczynski, J. F., & Rose, G. D. (1986) *Science (Washington, D.C.) 234*, 849–855.

Li, L., & Benkovic, S. J. (1991) *Biochemistry 30*, 1470–1478.

Middleton, S. A., Stebbins, J. W., & Kantrowitz, E. R. (1989) *Biochemistry 28*, 1617–1626.

Otting, G., Widmer, H., Wagner, G., & Wüthrich, K. (1986) *J. Magn. Reson. 66*, 187–193.

Pompliano, D. L., Peyman, A., & Knowles, J. R. (1990) *Biochemistry 29*, 3186–3194.

Poole, L. B., Loveys, D. A., Hale, S. P., Gerlt, J. A., Stanczyk, S. M., & Bolton, P. H. (1991) *Biochemistry 30*, 3621–3627.

Richardson, J. S. (1981) *Adv. Protein Chem. 34*, 167–339.

Sanger, F. (1981) *Science (Washington, D.C.) 214*, 1205–1210.

Seeger, D. R., Cosulich, D. B., Smith, J. M., & Hultquist, M. E. (1949) *J. Am. Chem. Soc. 71*, 1753–1758.

Stone, S. R., & Morrison, J. F. (1982) *Biochemistry 21*, 3757–3756.

Viola, R. E., Cook, P. F., & Cleland, W. W. (1979) *Anal. Biochem. 96*, 334–340.

Volz, K. W., Matthews, D. A., Alden, R. A., Freer, S. T., Corwin, H., Kaufman, B. T., & Kraut, J. (1982) *J. Biol. Chem. 257*, 2528–2536.

Williams, J. W., Morrison, J. F., & Duggleby, R. G. (1979) *Biochemistry 18*, 2567–2573.